DEVELOPMENT OF THREE-DIMENSIONAL MULTICELLULAR TISSUE-LIKE CONSTRUCTS FOR MUTATIONAL ANALYSIS USING MACROPOROUS MICROCARRIERS

JACQUELINE A. JORDAN, DENISE N. FRAGA, and
STEVE R. GONDA[1]

Universities Space Research Association, Division of Space and Life Sciences, Houston, TX 77058 (J.A.J.), Department of Chemistry and Biochemistry, University of Notre Dame, South Bend, IN, 46637 (D.N.F.), Cellular Biotechnology Program, NASA Johnson Space Center, Houston, TX 77058 (S.R.G.)

Running Title: 3-D TISSUE-LIKE CONSTRUCTS

[1]To whom correspondence should be addressed at Cellular Biotechnology Program, NASA Johnson Space Center, 2101 NASA Rd., 1, Houston, TX 77058. Telephone: 281-483-8745; Fax: 281-483-0402; E-mail: sgonda@ems.jsc.nasa.gov.

SUMMARY

A three-dimensional (3-D), tissue-like model was developed for the genotoxic assessment of space environment. In previous experiments, we found that culturing mammalian cells in a NASA-designed bioreactor, using Cytodex-3 beads as a scaffold, generated 3-D multicellular spheroids. In an effort to generate scaffold-free spheroids, we developed a new 3-D tissue-like model by coculturing fibroblast and epithelial cells in a NASA bioreactor using macroporous Cultispher-S™ microcarriers. Big Blue® Rat 2λ fibroblasts, genetically engineered to contain multiple copies (>60 copies/cell) of the *Lac I* target gene, were cocultured with radiosensitive human epithelial cells, H184F5. Over an 8-day period, samples were periodically examined by microscopy and histology to confirm cell attachment, growth, and viability. Immunohistochemistry and western analysis were used to evaluate the expression of specific cytoskeletal and adhesion proteins. Key cell culture parameters (glucose, pH, and lactate concentrations) were monitored daily. Controls were two-dimensional monolayers of fibroblast or epithelial cells cultured in T-flasks. Analysis of 3-D spheroids from the bioreactor suggests fibroblast cells attached to and completely covered the bead surface and inner channels by day 3 in the bioreactor. Treatment of the 3-day spheroids with dispase II dissolved the Cultisphers™ and produced multicellular, bead-less constructs. Immunohistochemistry confirmed the presence of vimentin, cytokeratin and E-cadherin in treated spheroids. Examination of the dispase II treated spheroids with transmission electron microscopy (TEM) also showed the presence of desmosomes. These results suggest that the controlled enzymatic degradation of an artificial matrix in the low shear environment of the NASA-designed bioreactor can produce 3-D tissue-like spheroids.

Key Words: three-dimensional, macroporous microcarrier, bioreactor, rotating-wall vessel, Lac I

INTRODUCTION

Radiation exposure is one of the major concerns associated with long term manned space travel (Obe, et al. 1997; Yang, et al. 1997; Setlow, 1999). During space missions, astronauts are exposed to a complex environment of ionizing radiation that includes trapped belt radiation, galactic cosmic rays (GCR) and radiation from solar particle events (Wilson, et al. 1995; Nachtwey and Yang, 1991). Numerous studies have shown that exposure to ionizing radiation may cause extensive DNA damage that is directly related to development of certain cancers (Wu, et al. 1997; Cadet, et al. 1995; Krain, 1991). For the health and safety of the astronauts, the biological effects of space radiation must be determined. This has proven to be difficult due to the extrapolation of physical measurements of radiation to the potential toxic effects on living organisms. In an effort to study the genetic hazards associated with space radiation, researchers are using NASA-designed bioreactor systems to develop various tissue equivalent models that have characteristics of normal tissues (Akins, et al. 1997; Duray, et al. 1997; Khaoustov, et al. 1999; Gonda, et al. 2001). The development of these *in vitro* models could play an important role in advancing our understanding of how cells and tissues respond to ionizing radiation.

Tissue engineering is a new and emerging field in which researchers use cultured cells in combination with various biomaterials to generate new organs and tissues (Mooney, 1999; Saltzman, 1997; Freed and Vunjak-Novakovic, 1997). This includes the development of 3-D macroscopic tissue assemblies by culturing cells on complex extracellular matrices (i.e. bioresorbable scaffolds and microcarrier beads) in a bioreactor to promote 3-D assembly

(Schrimpf and Friedl, 1993; Mitteregger, et al. 1999; Eiselt et al. 2000). The advantage of these tissue assemblies is that they can be multicellular which promotes differentiation. These multicellular, differentiated tissue assemblies may be used to study tissue responses to toxic chemicals and radiation. To support the development of such 3-D tissue constructs NASA, through its work at the Johnson Space Center, successfully designed the High Aspect Ratio Vessel (HARV) bioreactor. This rotating wall bioreactor is a horizontally rotated, fluid-filled culture vessel equipped with a large surface membrane for oxygen diffusion. The HARV bioreactor creates a low shear fluid culture environment and models microgravity conditions that allow for the development of 3-D cellular aggregation, differentiation, and growth (Jessup, et al. 1993; Duray, et al. 1997; Unsworth and Lelkes, 1998; Low, et al. 2001). Experimental studies have shown that the NASA-designed bioreactor promotes the 3-D growth of numerous normal and cancerous cell lines including skeletal muscle satellite cells, bovine chondrocytes, human and rat osteosarcoma cells, human liver cells, and human carcinoma cells (Rhee, et al. 2001; Licato, et al. 2001; Ingram, et al. 1997; Baker and Goodwin, 1997; Unsworth and Lelkes, 1998; Molnar, et al. 1997).

One of the methods used to attain differentiated tissue assemblies in the rotating wall bioreactor is to culture cells on resorbable polymeric scaffolds made of polymers such as fibrous polyglycolic acid (PGA) (Freed, et al. 1997). PGA and other polymer biomaterials are used as temporary scaffolds to promote cell attachment and aggregation. These scaffolds are biodegradable, but their usefulness is limited by the prolonged time required for complete degradation of the scaffold to form a scaffold-free tissue-construct. In this study, we used macroporous Cultispher-S™ beads to generate tissue culture assemblies (Cahn, 1990). These Cultispher-S™ beads are composed of a highly cross linked gelatin matrix and can be dissolved

with minimal damage to cell membranes using a neutral protease, like dispase II (Normand and Karasek, 1995; Warejcha, et al. 1996). Using this technique, Rat 2λ fibroblast cells, transfected with the *Lac I* gene as a target for mutagenesis, were cocultured with radiosensitive human epithelial cells on Cultispher-S™ macroporous beads. Cultispher-S™ beads, containing both cell types, are treated with dispase II to generate bead-less spheroids. Spheroids, following treatment in the low shear bioreactor, retain their 3-D structure and form multicellular, multilayer, tissue-like constructs as confirmed by ultrastructural and histochemical analysis of samples. In summary, we report the development of a new tissue-engineering model employing a mild protease to rapidly degrade the artificial scaffolding material while retaining a viable, tissue-like construct for mutational analysis.

MATERIALS AND METHODS

Cells and Culture Conditions

Big Blue® Rat 2λ fibroblasts were obtained from Stratagene, Inc. (Austin, TX). These cells are derived from a rat 2λ embryonic fibroblast cell line and genetically engineered to contain the Big Blue® λLIZ shuttle vector (~60 copies/cell) and a pSV2NEO plasmid that provides resistance to geneticin. Incorporated within the shuttle vector is the *Lac I* gene that is used as a target for mutagenesis. The shuttle vector also contains the α *Lac Z* gene that encodes the α-portion of the β-galactosidase. For subculturing, rat 2λ fibroblasts were grown in tissue culture flasks, passage 4-6, in Dulbecco's modified Eagle's medium (DMEM) supplemented with 10% fetal bovine serum (FBS), 50 U/ml of penicillin/streptomycin, 2 mM glutamine, and 200 μg/ml of geneticin (Sigma-Aldrich, St. Louis, MO). Human epithelial cells (H184B5FM10) were obtained from Dr.

Durante at the University "Federico II", Naples, Italy, and are a growth variant of a primary culture of mammary cells generated by Dr. M. Stampfer at Lawrence Berkeley Laboratory, Berkeley, CA. These cells were found to be immortalized, non-tumorgenic, contact-inhibited, and exhibit both anchorage and serum dependent growth. These cells were cultivated in tissue culture flasks; passage 41-43, in αMEM supplemented with 10% FBS, 50 U/ml penicillin/streptomycin, 2 mM glutamine, and 1.25 μg of fungizone. Both cell lines were maintained in a humidified incubator at 37°C and 95% atmospheric air/5% CO_2. All cell culture supplies, unless otherwise noted, were purchased from Invitrogen (Carlsbad, CA).

Bioreactor

The non-perfused, horizontally rotated, 50 ml HARV bioreactor was supplied by Synthecon, Inc. (Houston, TX). This vessel provides a low shear fluid environment for the suspension of cells and tissues and contains a silicon permeable membrane to allow oxygen to diffuse, bubble free, into the culture medium. Bioreactors inoculated with cells and beads were placed in an incubator and rotated to suspend cells and aggregates (10-12 rpm). Sterile conditions were maintained during sampling and media feedings (Figure 1).

Microcarriers

Highly cross linked macroporous gelatinous beads, Cultispher-S™, were used as the microcarriers for cell attachment and purchased from Hyclone Laboratories (Logan, UT). They have a size distribution (wet) of 130-380 μm and a pore size of 20 μm. Cultispher-S™ was provided as a white, dry granular powder and prepared for cell culture by hydration and

autoclaving in Ca^{2+} and Mg^{2+} free phosphate buffered saline (PBS). Sterile beads were washed twice in culture medium and stored hydrated at 4°C for subsequent use.

Experimental Design

A schematic showing the experimental design for the development of 3-D, multicellular, tissue-like spheroids is shown in Figure 2. Exponentially growing rat 2λ fibroblasts were trypsinized, washed in PBS, and cultured with Cultispher-S™ beads in sterile suspension culture dishes (100 mm x 20 mm) at a 100:1 cell to bead ratio, as recommended by the manufacturer. Each culture dish was seeded with 1.0×10^3 beads/ml, and 1.0×10^5 fibroblast cells/ml, and placed on a rotary shaker (10-12 rpm) in a 37°C tissue culture incubator. Following a 4-day incubation, Cultispher-S™ beads with attached fibroblast cells were inoculated into the HARV bioreactor and incubated over an 8-day period. Three different HARV culture conditions were examined: Rat 2λ fibroblasts only (monoculture), Rat 2λ fibroblasts with the addition of 1.0×10^5 human epithelial cells/ml added at day 1 (coculture), and a coculture subsequently treated with 0.1 U/ml of 1x Dispase II (Roche) 4 and 6 days after inoculation in the bioreactor (dispase treated). Samples of culture media from each experiment were monitored daily for glucose consumption, pH, and lactic acid production using a Blood Gas Analyzer (Bayer Diagnostics, Tarrytown, NY). Cell samples were taken throughout the experiment to assess viability using MTT (3-{4,5-dimethylthiazol-2-yll-2,5-diphenyltetrazolium bromide). The incubation of MTT with live cells generates a highly visible blue product.

Histology and Immunohistochemistry

Samples were fixed in Omnifix II for 4 hours at 4°C (An-Con Genetics, Melville, NY), washed in 0.1 M cacodylate buffer, dehydrated, embedded in paraffin, and thin sections were prepared on slides. For general histology, slides were deparaffinized and stained with hematoxylin and eosin or Movat. For immunohistochemistry, slides were deparaffinized and antigenic sites exposed using the microwave citrate pretreatment method. Slides were then incubated in 0.3% hydrogen peroxide for 30 minutes and washed twice with PBS containing 0.05% Triton-X, and blocked with PBS containing horse serum using a Vectastain Kit supplied by Vector Laboratories (Burlingame, CA). Monoclonal antibodies to vimentin and cytokeratins pan, 7, 8, and 18 were obtained from Oncogene Research Products (San Diego, CA). Anti-E-cadherin antibodies were obtained from Chemicon (Temecula, CA). Antibody binding was visualized using a peroxidase-conjugated anti-IgG antibody and 3,3-diaminobenzidine (DAB) (Kirkegaard & Perry Laboratories, Gaithersburg, MD). Slides were counterstained using hematoxylin or methyl green. To examine cell monolayers, cells were grown directly on microscope slides, washed in PBS, and fixed in -20°C methanol for 20 minutes and stained accordingly.

Western Blot Analysis

In order to detect vimentin, cytokeratins, and E-cadherin in total cell extracts, cells were washed in PBS and lysed directly in PBS containing 0.1% sodium dodecyl sulfate (SDS), 1% NP40, and 1% sodium deoxycolate. Protein concentrations were determined using the micro BCA protein assay supplied by Pierce Chemical Company (Rockford, IL). Samples were vortexed and boiled for 10 minutes in SDS sample buffer containing β-mercaptoethanol. Gel electrophoresis of proteins was performed using a 12% SDS-polyacrylamide gel as described by Laemmli. Proteins were transferred from a gel to nitrocellulose filters, blocked with 5% milk in Tris

Buffered Saline (TBS) containing 0.1% Tween. The nitrocellulose filter with attached protein was then incubated with the appropriate monoclonal antibody. Primary antibodies were visualized by peroxidase-conjugated anti-IgG antibodies and ECL detection reagents (Amersham, Piscataway, NJ).

Electron Microscopy

Samples for scanning electron microscopy (SEM) were fixed in 2% glutaraldehyde and 2% paraformaldehyde in 0.1 M cacodylate buffer for 4-6 hrs at 4°C and washed in 0.1 M cacodylate buffer. Fixed samples were then dehydrated, critical point dried, and coated by gold sputtering for examination. Transmission electron microscopy (TEM) samples were fixed in the same manner as SEM samples, post-fixed in 1% Osmium Tetraoxide and En-Bloc stained with 2% Uranyl Acetate. Specimens were dehydrated by graded ethanol, and embedded in Polybed/812 resin. Both thick and thin sections were cut on Reichert Ultracut S microtome. Seventy nanometer thin sections were stained by modified Reynolds Lead Citrate and examined using a Philips CM100 Electron Microscope.

RESULTS

Attachment of Fibroblast Cells to Macroporous Beads incubated in Suspension Culture Dishes

Figure 3 summarizes the microscopic observations confirming the growth and attachment of fibroblast cells on macroporous beads. Using a phase contrast microscope, we observed the porous and sponge-like structure of the Cultispher-S™ macroporous beads before seeding with fibroblast cells, as shown in Figure 3A. Since the Cultispher-S™ beads are uncharged, the

attachment of cells to the macroporous beads was initially dependent upon the absorption of serum proteins, such as fibronectin onto the bead surface. In this study, to facilitate the attachment of the fibroblast cells to the beads, we incubated cultures for 4 days in suspension culture dishes on a laboratory shaker (15 rpm). Our results show that within 48 hours over 95% of the fibroblast cells attached to the macroporous beads. To determine if cell attachment and growth was limited to the bead surface or included the internal portion of the bead, paraffin-embedded thin sections were analyzed using histology. Hematoxylin and eosin (H&E) staining of samples from day 3 on the shaker confirmed the presence of a monolayer of cells on the surface of the bead and growth toward the inner portion of the bead (Figure 3B). We also examined samples during this 4-day culture period for the production of extracellular matrix components (ECM) such as collagen. Movat staining of day 4 cultures confirmed the deposition of collagen in 3-D spheroids (Figure 3C). Also note the Movat staining of intact cell nuclei (black) and the extensive black staining of the macroporous bead. With the use of SEM, we examined the localization of cells on the macroporous beads. Cells were observed on the bead surface and entering pores leading to the internal channels (Figure 3D). TEM was valuable in confirming the adherence of fibroblast cells to the bead surface (Figure 3E). High cell viability of fibroblast cells cultured with beads on a rotary shaker was observed following incubation with MTT (Figure 3F).

Growth and Metabolism of Spheroids Cultivated in the HARV Bioreactor

Following a 4-day incubation period on a laboratory shaker, Cultispher-S™ beads, with attached fibroblasts, were cultivated in the bioreactor without (monoculture) or with (coculture) the addition of human epithelial cells. Figure 4 shows the staining of representative spheroids taken

from the control monoculture and the control coculture (untreated) bioreactors over the 8-day culture period. Fibroblast cells (monoculture) maintained their attachment to the surface of the beads and grew within pores by day 3 in the HARV in Figure 4A. In addition, Movat staining reveals densely packed cells within pores and the continued secretion of newly formed, yellow-stained collagen in bioreactor-derived samples (Figure 4B). At day 8, we observed mitotic cells in the internal portion of the bead suggesting active cell division (Figure 4C). Both H&E and Movat staining of spheroids containing a coculture of fibroblast and epithelial cells cultivated in the bioreactor reveal evenly distributed cells layered in the orifices of the bead (Figure 4D and E). At day 8, Movat staining clearly confirmed the presence of newly formed collagen in the center of the coculture spheroids incubated in the bioreactor (Figure 4F).

We also monitored the culture conditions in the bioreactor during dispase II treatment and spheroid formation (Figure 5). Media samples were withdrawn daily to monitor glucose concentration, pH levels, and lactic acid production. Comparison of the glucose consumption and lactic acid production in the bioreactor cultures to that in fresh pre-warmed media suggest active metabolism occurring within spheroids (Figures 5A and B). We did not observe any significant differences in glucose consumption, lactic acid production, and pH levels between untreated and dispase treated bioreactor cultures. All cultures were fed daily to maintain glucose values above 100 mg/dL throughout the experiment.

Analysis of Spheroids following Dispase Treatment in the HARV

Figure 6 shows results following the treatment of spheroids with dispase II. Coculture spheroids in the bioreactor were treated with dispase II to dissolve the macroporous bead on days 4 and 6. Toludine staining of spheroids following the 1st dispase treatment shows a partial degradation of

the bead infrastructure while maintaining important cell-to-cell connections (Figure 6A). Toludine stains cells light purple and the macroporous bead black. MTT staining of spheroids following the 1st Dispase treatment shows purple-blue staining of cells that is indicative of cell viability (Figure 6B). Detachment of cells from the Cultispher-S™ bead while maintaining cellular integrity after the 1st dispase treatment is confirmed by TEM (Figure 6C). Phase contrast microscopy of spheroids show that cells retained the 3-D architecture following the complete dissolution of the Cultispher-S™ bead by a 2nd treatment with dispase II (Figures 6D and 6E). Intense MTT staining confirmed that cellular viability was maintained following the 2nd dispase treatment and one week of culture in the bioreactor (Figure 6F). Analysis of samples by H&E staining confirm the complete digestion of the Cultispher-S™ bead after the 2nd dispase treatment and the retention of a multilayer of cells with a loose 3-D appearance (Figures 6G and 6H). TEM confirmed the 3-D tissue-like arrangement of the cells and the absence of the bead (Figure 6I). Spheroids that were cultured in the HARV for one-week after the 2nd dispase treatment still retained the 3-D architecture (Figure 6J), tissue-like organization, and prominent collagen containing ECM (Figures 6K and 6L).

Expression of Cytoskeletal and Adhesion Proteins

The immunohistochemical staining of spheroids were useful in identifying cell types and evaluating the interaction of epithelial and fibroblast cells in culture. Figure 7A shows the elongated appearance of fibroblast cells grown in two-dimensional (2-D) monolayers. Fibroblast cell monolayers were immunostained for the presence of vimentin, a Type III intermediate filament protein normally expressed in cells of mesenchymal origin. Figures 7B and 7C show immunostained areas within the cytoplasm of the fibroblasts that are indicative of vimentin

expression. Counterstaining using Hematoxylin stains the nucleus light blue. Monolayers of epithelial cells, used as a negative control, were not immunoreactive with anti-vimentin antibody (data not shown). Confluent monolayers of cuboidal shaped human epithelial cells are shown in Figure 7D. Immunohistochemical staining of epithelial cells with a pan-cytokeratin antibody confirms the presence of cytokeratin proteins in the cytoplasm of these cells (Figures 7E and 7F). Monolayers of fibroblast cells, used as a negative control, were not immunoreactive for anti-cytokeratin. Figures 7G and 7H show the immunohistochemical staining of epithelial cell monolayers with an antibody to the cell adhesion molecule E-cadherin. E-cadherin staining was localized in the cellular junctions between epithelial cells.

We observed the continued expression of cytoskeletal and adhesion proteins in monoculture and coculture spheroids grown in the HARV bioreactor. Figures 8A and 8B show a cross section of 3-day old fibroblast monoculture spheroids stained for vimentin. The expression of vimentin was detected throughout the macroporous bead suggesting the presence of intact fibroblast cells. Dispase treated monoculture spheroids grown in the HARV also show intense anti-vimentin antibody staining (Figure 8C). Notice the development of the tissue-like organization of the spheroid and the absence of the Cultispher-S™ bead. Figure 8D shows a coculture spheroid incubated in the bioreactor for 3 days. Immunostaining with anti-vimentin detected the presence of fibroblasts in coculture spheroids. Immunoreactive vimentin was also detected in dispase treated coculture spheroids (Figures 8E and 8F). Note the presence of unstained cells in coculture spheroids presumed to be epithelial cells (Figures 8D, 8E, and 8F). Analysis of spheroids stained for pan-cytokeratin indicates the presence of epithelial cells between beads (Figure 8G). Higher magnification of spheroids shows the presence of cytokeratin in the cytoplasm of epithelial cells, as seen in Figure 8H. Importantly, dispase II

treatment did not alter the cytokeratin expression in epithelial cells (Figure 8I). Differential immunostaining for vimentin and cytokeratin confirmed the presence and location of both cell types. Coculture spheroids were also immunostained for E-Cadherin. Our results show the immunoreactivity of E-Cadherin in the periphery of coculture spheroids (Figure 8J).

We confirmed the cross reactivity of the antibodies used for immunohistochemistry in Figure 9. Cell lysates of fibroblast or epithelial cells were immunostained for vimentin and various cytokeratins. Vimentin was found to be a 57 kDa protein highly expressed by rat 2λ fibroblast cells. Cytokeratin content in epithelial tissues varies and is dependent on the type and degree of differentiation of the cells. The epithelial cells used in this study were immunoreactive to cytokeratin 7 with a molecular weight of 54 kDa, cytokeratin 8 with a molecular weight of 53 kDa and cytokeratin 18 with a molecular with a molecular weight of 45 kDa. E-cadherin antibody reacts with a 120kDa transmembrane glycoprotein found in the adherens junction of epithelial cells.

Electron Microscopy Analysis of Spheroids

SEM and TEM were used to (i) monitor the attachment and distribution of cells on the bead surface and in channels, (ii) study the formation and fate of the 3D cell-ECM architecture prior to and after bead degradation by dispase, and (iii) characterize the morphology and differentiation of control and enzyme-treated spheroids, including cell specific and tissue morphological markers. Specimens examined included both spheroids comprised only of fibroblasts (monoculture) and spheroids with both fibroblast and epithelial cells (coculture). Figure 10A shows numerous spheroids formed by monoculture with fibroblasts completely covered with fibroblasts and their distribution (Figure 10B) on the bead surface and into the bead

pores and channels. Monoculture spheroids that were treated twice with dispase and incubated for one week in the HARV bioreactor showed a loose 3-D network of cells with clear demarcations between cells and little ECM (Figure 10C). This was confirmed by TEM that shows the absence of the bead infrastructure (Figure 10D). Figure 11A shows spheroids formed by coculture with fibroblasts and epithelial cells, treated twice with dispase, and cultured for one week in the HARV bioreactor after enzyme treatment. The bead surfaces are completely covered by a well-organized and integrated cell-ECM layer. In Figure 11B, we observed the presence of microvilli and desmosomes as shown by TEM. Desmosomes are connecting sites for intermediate filaments and act to distribute tensile forces throughout the cell. Desmosomes link adjoining cells to each other and are used routinely as a marker for the presence of differentiated epithelial cells. Desmosomes, consisting of two dense plaques on opposing cell surfaces, were observed as a button-like structure in transmission electron micrographs (Figure 11C) of one-week coculture spheroids. Analysis of epithelial cells cultured on Cytodex-3 microcarrier beads, as a positive control, confirms the presence of cells with desmosome connections in 3-D culture (Figures 11D and 11E). Figure 11F shows the layering of epithelial cells on charged microcarriers. Observe the spatial orientation of an epithelial cell interacting with attached epithelial cells.

DISCUSSION

Multicellular tissue-like models are valuable in determining the biological response of cells to potentially toxic agents and in the extrapolation of these responses to humans and various animal models (Meli, et al. 1999; Goodhead, et al. 1995; Mueller-Klieser, 1987). In this study, our goal was to develop a fast and efficient method to produce beadless, multicellular, tissue-like

constructs by enzymatically degrading the scaffold while retaining the 3-D architecture. Cultispher-S™ beads were used as a scaffold for the attachment and growth of fibroblast and epithelial cells on the bead surface and within bead channels. After the early formation of the 3-D infrastructure, samples were treated in the HARV with dispase II to slowly degrade the scaffold. Dispase treatment was completed in less than one week and resulted in a fairly uniform population of tissue-like beadless spheroids. These tissue-like characteristics were confirmed by electron microscopy, histology, and immunohistochemistry and were proven to be more tissue-like than other models cultured on plastic (Spendlove, 1995; Saltzman, 1997).

We used cell lines previously described by this lab to produce multicellular tissue-like constructs when cultured on Cytodex-3 microcarriers in the HARV bioreactor. The Big Blue® rat cell line (Rat 2λ) is useful for *in vitro* mutagenesis studies. The cell line is transfected with the lambda/LIZ shuttle vector that contains the *lacI* and *alpha Lac Z* genes used over the years for various toxicological applications (Gorelick, 1995; Kohler, 1991). The human mammary epithelial cell line (H184B5) was developed for studying neoplastic transformation *in vitro*. It is a growth variant obtained from heavy ion irradiated immortal mammary cells. Other researchers have used this human epithelial growth variant as a model to determine the possible carcinogenic effects of space radiation (Yang, 1994; Durante, 1995).

In this study, Cultispher-S™ beads were used as the scaffold for the attachment and growth of rat 2λ fibroblast and human epithelial cells. Previous studies from several laboratories have shown that normal and cancerous cell types attached to and populated the Cultispher-S™ macroporous beads. Some examples include Chinese hamster ovary, green monkey kidney, and human lung carcinoma cells (Werner, et al. 2000; Maurer, et al. 1999; Rasey, et al. 1996; Nikolai and Hu, 1992). As revealed by our light and electron microscopy observations, Rat 2λ fibroblast

cells attached to the bead surface and readily populated the internal and external portions of the beads. Following the initial attachment of the fibroblasts to beads, cells grew to very high densities and high cell viability was observed by MTT staining. We also examined the attachment and growth of human epithelial cells alone on Cultispher-S™ macroporous microcarriers. Interestingly, the epithelial cells, in the absence of fibroblast cells, did not bind to and populate the beads in the same manner as the fibroblast cells. Epithelial cells attached to a few areas on the macroporous bead. These data suggest that the epithelial cells are not as efficient as the fibroblast cells in binding to uncharged, uncoated macroporous beads. We believe this is either due to insufficient amounts of fibronectin or another ECM component (collagen, laminins, or proteoglycans) in the media or secreted by fibroblast cells.

Numerous studies suggest epithelial attachment, proliferation and differentiation is highly dependent on cellular interaction with fibroblast cells (Darcy, et al. 2000; Deugnier, et al. 1999). Previously, we have shown that human epithelial cells readily attached to Type III collagen-coated Cytodex-3 beads. Epithelial cells attached to Cytodex-3 beads in the presence of serum, but are localized primarily to areas between beads (unpublished data). Some studies conclude normal epithelial cell growth increased when cells were exposed to fibroblast cells or supernatants (Gache, et al. 1998; Young and Adamson; 1993). Cocultures of NIH 3T3/J2 fibroblasts and primary human keratinocytes on small intestinal submucosa in 3-D allows for cell migration and spatial organization (Badylak, et al. 1998). Cocultures of normal small intestinal mesenchymal cells with normal small intestinal epithelial cultivated on Cytodex-3 beads, in the NASA-designed low shear bioreactors, yielded aggregates with differentiated epithelial cells, ECM and basal lamina (Goodwin, et al. 1993). In some studies, mammary epithelial cell morphogenesis and differentiation was dependent on the formation of a basement membrane and

loss of ECM components was associated with perturbations in cell adhesion (Weaver, et al. 1997). We found in this study that seeding the macroporous beads first with fibroblast cells for 4 days stimulated the subsequent binding of epithelial cells generating a multicellular tissue-like spheroid model. Histochemical analysis suggest this may be due to the secretion of ECM components, like collagen, from resident fibroblast cells.

We also determined if dispase II was successful in dissolving the Cultispher-S™ bead while the integrity of the developed ECM was maintained. Many researchers have used dispase II for tissue disaggregation and subcultivation procedures (Nguyen, et al. 1993; Warejcka, et al. 1996; Normand and Karasek, 1995). This protease has been used at specific concentrations to prevent clumping of suspension cell culture and to separate intact epidermis sheets in culture from substratum (Van Dorp, et al. 1999). Dispase II has been reported to cause minimal damage to cell membranes while maintaining high cell viability and recommended for the digestion of Cultispher-S™ beads yielding free dissociated cells (Matsumura, et al. 1975; Takashima and Grinnell, 1984). We report the establishment of a method to dissolve the Cultispher-S™ bead in a low fluid shear environment while maintaining overall 3-D organization including cell/cell interactions and cell/ECM organizations. After the Cultispher-S™ beads were populated with both fibroblast and epithelial cells and the 3-D tissue/ECM established we intermittently dissolved the bead with low doses of dispase II. During treatment, cells continued to grow, interact, and develop a prominent ECM. Light and electron microscopy observations confirm that we were successful in dissolving the Cultispher-S™ bead while maintaining structural integrity and cellular viability.

The multicellular spheroids produced by our method have structural characteristics of normal *in vivo* tissue. This was confirmed by examining the presence of intermediate filaments

and adhesion molecules. Intermediate filament proteins are a subset of cytoskeletal proteins important in stabilizing organelles and contributing to cell mobility (Jansen, et al. 1997). Cytokeratin intermediate filaments are found in epithelial cells attached to specialized cell junctions. Vimentin intermediate filaments are found in cells of mesenchymal origin like fibroblasts. We examined our 3-D spheroids to determine the presence (cellular distribution and localization) of intermediate filaments. Our results confirm the immunohistochemical staining of fibroblasts by a monoclonal antibody to vimentin, a type III intermediate filament. Epithelial cells were detected using a pan antibody that detects cytokeratins 4-8, 10, 13-16, 18 and 19. The reactivity of cytokeratin and vimentin antibodies confirms of the presence of both cell types in our multicellular spheroid model. The formation of a tissue is also dependent on adequate cellular adhesions. We examined our spheroids for the presence of cadherins that mediate Ca^{2+} dependent cell-cell adhesion between epithelial cells in vertebrate tissues. As reported by others, we observed the presence of E-cadherin in monolayer of epithelial cells and in multicellular spheroids (Gordon, K.E., et al. 2000)

Specialized cell junctions occur at many points in all tissues, and they are very important to the function of epithelial cells (Stein, 1993). Through desmosomes, the intermediate filaments of adjacent cells are connected to form a continuous network throughout the tissue. They play a key role in epithelial cell adhesion by binding cells together and linking intermediate filament networks. Using TEM, we observed the presence of desmosomes in our developed multicellular spheroids that is indicative of epithelial cell differentiation.

In future studies we will use these multicellular tissue-like spheroids to evaluate the mutagenic effects of space radiation. It is important to evaluate the risk associated with long-term exposure to space radiation. This is especially true for epithelial cells that line a significant

portion of the human body and have proven to be susceptible to toxic insult (Rodriguez-Boulan and Nelson, 1989; Yang and Craise, 1994). In conclusion, the development of new multicellular tissue-like models for the genotoxic assessment of space environments would provide valuable data to assess the harmful effects of radiation to humans.

ACKNOWLEDGMENTS

The authors wish to thank Julie Wen, Department of Pathology, University of Texas Medical Branch for her assistance with the preparation and analysis of samples for electron microscopy; and Sharon K. Jackson for her help in preparing the manuscript. This research was supported by grants from the National Aeronautics and Space Administration NRA-98-HEDS-02.

REFERENCES

Akins, R. E.; Schroedl, N. A.; Gonda, S. R.; and Hartzell, C. R. Neonatal Rat Heart Cells Cultured in Simulated Microgravity. In Vitro Cell. Dev. Biol - Animal 33:337-343; 1997.

Badylak, S. F.; Record, R.; Lindberg, K.; Hodde, J.; Park, K. Small intestinal Submucosa: A substrate for In Vitro Cell Growth. J. Biomater. Sci. Polym Ed. 9:8:863-78; 1998.

Baker, T. L.; Goodwin, T. J. Three-Dimensional Culture of Bovine Chondrocytes in Rotating-Wall Vessels. In Vitro Cell. Dev. Biol – Animal 33:358-365; 1997.

Cadet, J.; Girault, I.; Gromova, M.; Molko, D. Effects of heavy ions on nucleic acids: measurement of the damage. Radiat. Environ. Biophys. 34:55-57; 1995.

Cahn, F. Biomaterials Aspects of Porous Microcarriers for Animal Cell Culture. TIBTECH 8:131-136; 1990.

Darcy, K. M.; Zangani, D.; Shea-Eaton, W.; Shoemaker, S. F.; Lee, P. H.; Mead, L. H.; Mudipalli, A.; Megan, R.; IP, M. M. Mammary Fibroblasts Stimulate growth, Alveolar Morphogenesis, and Functional Differentiation of Normal Rat Mammary Epithelial Cells. In Vitro Cell. Dev. Biol. - Animal 36:578-592; 2000.

Deugnier, M. M.; Faraldo, P.; Rousselle, J.P.; Thiery; Glukhova, M. A. Cell-extracellular matrix interactions and EGF are important regulators of the basal mammary epithelial cell phenotype. Journal of Cell Science 112:1035-1044; 1999.

Durante, M.; Grossi, G.; Gialanella, G.; Pugliese, M.; Nappo, M.; Yang, T. C. Effects of alpha-particles on Survival and Chromosomal Aberrations in Human Mammary Epithelial cells. Radiat. Environ. Biophys. 34:195-204; 1995.

Duray, P.H.; Hatfill, S. J.; Pellis, N. R. Tissue Culture in Microgravity. Science and Medicine. May/June: 46-55; 1997.

Eiselt, P.; Yeh, J.; Latvala, R. K.; Shea, L. D.; Mooney, D. Porous carriers for biomedical applications based on alginate hydrogels. Biomaterials 21:1921-1927; 2000.

Freed, L. E.; Vunjak-Novakovic, G. Microgravity Tissue Engineering. In Vitro Cell. Dev. Biol. - Animal 33:381-385; 1997.

Freed, L. E.; Langer, R.; Martin, I.; Pellis, N. R.; Vunjak-Novakovic, G. Tissue engineering of cartilage in space. Proc. Natl. Acad. Sci. 94:13885-13890; 1997.

Gache, C.; Berthois, Y; Martin, P; Saez, S. Positive Regulation of Normal and Tumoral Mammary Epithelial Cell proliferation by Fibroblasts in Coculture. In Vitro Cell. Dev. Biol. - Animal 34:347-351; 1998.

Gonda, S. R.; Wu, H.; Pingerelli, P. L.; Glickman, B. W. Three-Dimensional Transgenic Cell Model to Quantify Genotoxic Effects of Space Environment. Adv. Space Res. 27:2:421-430; 2001.

Goodhead, D. T. Molecular and cell models of biological effects of heavy ion radiation. Radiat. Environ. Biophy. 34:2: 67-72; 1995.

Goodwin, T. J.; Schroeder, W. F.; Wolf, D. A.; Moyer, M. P. Rotating-Wall Vessel Coculture of Small Intestine as a Prelude to Tissue Modeling: Aspects of Simulated Microgravity. Proceeding of Society for Experimental Biology and Medicine 202:181-192; 1993.

Gordon, K. E.; Binas, B.; Chapman, R. S.; Kurina, K. M.; Clarkson, R. W.; Clark, A. J.; Lane, E. B.; Watson, C. J. A Novel Cell Culture Model for Studying Differentiation and Apoptosis in the Mouse Mammary Gland. Breast Cancer Res. 2:222-235; 2000.

Gorelick, N. J. Overview of mutation assays in transgenic mice for routine testing. Environ. Mol. Mutagen 25:3:218-30; 1995.

Ingram, M.; Techy, G. B.; Saroufeem, R.; yazan, O.; Narayan, K. S.; Goodwin, T. J.; Spaulding, G. F. Three-Dimensional Growth Patterns of Various Human Tumor Cell Lines in Simulated Microgravity of a NASA Biorector. In Vitro Cell Dev. Biol - Animal 33:459-466; 1997.

Jessup, J. M.; Goodwin, T. J.; Spaulding, G. Prospects for Use of Microgravity-Based Bioreactors to Study Three-Dimensional Host-Tumor Interactions in Human Neoplasia. Journal of Cellular Biochemistry 51:290-300; 1993.

Jansen, J. A.; den Braber, E. T.; Walboomers, X. F.; duRuijter. J. E. Soft Tissue and Epithelial Models. Adv. Dent. Res. 13:57-66; 1999.

Khaoustov, V.; Darlington, G. J.; Soriano, H. E.; Krishnan, B.; Risin, D.; Pellis, N.; Yoffe, B. In Vitro Cell. Dev. Biol - Animal 35:501-509; 1999.

Kohler, S. W.; Provost, G. S.; Fieck, A.; Kretz, P. L.; Bullock, W. O.; Sorge, J. A.; Putman, D. L.; Short, J. M. Spectra of Spontaneous and Mutagen-induced mutations in the lacI gene in transgenic mice. Proc. Natl. Acad. Sci. 88:18:7958-62; 1991.

Krain, L. S. Aviation, High Altitude, Cumulative Radiation Exposure and their Associations with Cancer. Medical Hypotheses 34:33-40; 1991.

Licato, L. L.; Prieto, V. G.; Grimm, E. A. A Novel Preclinical Model of Human Malignant Melanoma Utilizing Bioreactor Rotating-Wall Vessels. In Vitro Cell. Dev. Biol. - Animal 37:121-126; 2001.

Low, H. P.; Savarese, T. M.; Schwartz, W. J. Neural Precurosor Cells Form Rudimentary Tissue-Like Structures in a Rotating-Wall Vessel Bioreactor. In Vitro Cell. Dev. Biol - Animal 37:141-147; 2001.

Matsumura, T.; Nitta, K.; Yoshikawa, M.; Takaoka, T.; Tatsuta, H. Action of bacterial neutral protease on the dispersion of mammalian cells in tissue culture. Japan J. Exp. Med. 45:5:383-92; 1975.

Maurer, B. J.; Ihnat, M. A.; Morgan, C.; Pullman, J.; O'Brien, C.; Johnson, S. W.; Rasey, J. S.; Cornwell, M. M. Growth of human Tumor Cell in macroporous Microcarriers Results in o53-Independent, Decreased Cisplatin Sensitivity Relative to Monolayers. Molecular Pharmacology 55:938-947; 1999.

Meli, A.; Perrella, G.; Curcio, F.; Ambesi-Impiombato, F. In Vitro Cultured Cells as Probes fro Space Radiation Effects on Biological Systems. Mutat. Res. 430:2:229-34; 1999.

Mitteregger, R.; Vogt, G.; Rossmanith, E.; Falkenhagen, D. Rotary Cell Culture System (RCCS): A new method for Cultivating Hepatocytes on Microcarriers. The International Journal of Artificial Organs 22:12: 816-822; 1999.

Molnar, G.; Schroedl, N. A.; Gonda, S. R.; Hartzell, C. R. Skeletal Muscle Satellite Cells Cultured in Simulated Microgravity. In Vitro Cell. Dev. Biol. - Animal 33:386-391; 1997.

Mooney, D. J.; Mikos, A. G. Growing New Organs. Scientific American. April: 60-72; 1999.

Mueller-Klieser, W. Multicellular spheroids. J. Cancer Res. Clin. Oncol. 113:101-122; 1987.

Nachtwey, D. S.; Yang, T. C. Radiological Health Risks for Expoloratory Class Missions in Space. Acta. Astronaut. 23: 227-31; 1999.

Nikolai, T.J.; Hu, W. Cultivation of Mammalian Cells on Macroporous Microcarriers. Enzyme Microb. Technol. 14:203-208; 1992.

Normand, J.; Karasek, M. A Method for the Isolation and Serial Propagation of Keratinocytes, Endothelial Cells, and Fibroblasts from a Single Punch Biopsy of Human Skin. In Vitro Cell. Dev. Biol. - Animal 31:447-455; 1995.

Nguyen, B. T.; Thompson, J. S.; Sharp, J. D. Comparison of Techniques for Harvesting Enterocytes for Transplantation. Jour. of Surg. Res. 54:157-162; 1993.

Obe, G.; Johannes, I.; Johannes, C.; Hallman, K.; Reitz, G.; Facius, R. Chromosomal aberrations in blood lymphocytes of astronauts after long-term space flights. Int. J. Radiat. Biol. 72:6:727-734; 1997.

Rasey, J. S.; Cornwell, M. M.; Maurer, B. J.; Boyles, D. J. S.; Hofstrand, P.; Chin L.; Cerveny, C. Growth and radiation response of cells grown in macroporous gelatin microcarriers (CultiSpher-G^{TM}). Br. J. Cancer Suppl. 27:S78-81; 1996.

Rhee, H. W.; Zhau, H. E.; Pathak, S.; Multani, A. S.; Pennanen, S.; Visakorpi, T.; Chung, L. Permanent Phenotypic and genotypic Changes of Prostate Cancer Cells Cultured in a Three-Dimensional Rotating-Wall Vessel. In Vitro Cell. Dev. Biol - Animal 37:127-140; 2001.

Rodriguez-Boulan, E.; Nelson, W. J. Morphogenesis of the Polarized Epithelial Cell Phenotype. Science 245:718-725; 1989.

Saltzman, W. M. Weaving cartilage at zero g: the reality of tissue engineering in space. Proc. Natl. Acd. Sci. 94:13380-13382; 1997.

Schrimpf, G.; Friedl, P. Growth of human vascular endothelial cell on various types of microcarriers. Cytotechnology 13:203-211; 1993.

Setlow, R. B. The U.S. National Research Councils Views of the Radiation Hazard in Space. Mutat. Res. 436:2:169-75; 1999.

Spendlove, R. S. Culturing Cells that Maintain In Vivo Characteristics. Hyclone-Art to Science 14:1:1-2; 1995.

Stein, L. S.; Stein, D. W.; Echols, J.; Burghardt, R. C. Concomitant Alterations of Desmosomes, Adhesiveness, and Diffusion through Gap Junction Channels in a Rat Ovarian Transformation Model System. Experimental Cell Research 207:19-32; 1993.

Unsworth, B. R.; Lelkes, P. I. Growing tissues in microgravity. Nature Medicine 4:8:901-907; 1998.

Van Dorp, A.; Verhoeven, M.; Van Der Nat, T.; Koerten, H.; Ponec, M. A modified culture system for epidermal Cells for Grafting Purposes: An in Vitro and In Vivo Study. Wound Rep. Reg. 7:214-225; 1999.

Warejcka, D. J.; Harvey, R.; Taylor, B. J.; Young, H.; Lucas, P. A Population of Cells Isolated from Rat Heart Capable of Differentiation into Several Mesodermal Phenotypes. Jour. of Surg. Res. 62:233-242; 1996.

Weaver, V. M.; Fischer, A. H.; Peterson, O. W.; Bissell, M. J. The importance of the microenvironment in breast cancer progression: recapitulation of mammary tumorigenesis using a unique human mammary epithelial cell model and a three-dimensional culture assay. Biochem. Cell. Biol. 74:833-851; 1996.

Werner, A.; Duvar, S.; Muthing, J.; Buntemeyer, H.; Lunsdorf, H.; Strauss, M.; Lehmann, J. Biotechnology and Bioengineering 68:1:59-70; 2000.

Wilson, J. W.; Kim, M.; Schimmerling, W.; Badavi, F. F.; Thibeault, S. A.; Cucinotta, F. A.; Shinn, J. L.; Kiefer, R. Issues in Space Radiation Protection: Galactic Cosmic rays. Health Phys. 68:1:50-58; 1995.

Wu, H.; Durante, M.; George, K.; Yang, T. Induction of Chromosome Aberrations in Human Cells by Charged Particles. Radiation Research 148:S102-S107; 1997.

Yang, C. H.; Craise, L. M. Development of Human Epithelial Cell Systems for Radiation Risk Assessment. Adv. Space Res. 14:10:10:115-10:120; 1994.

Yang, C. H.; Craise, L. M.; Durante, M.; Mei, M. Heavy-Ion Induced Genetic Changes and Evolution Processes. Adv. Space Res. 14:10:373-382; 1994.

Yang, T. C.; Mei, M.; George, K. A.; Craise, L. M. DNA Damage and Repair in Oncogenic Transformation by Heavy Ion Radiation. Adv. Space Res. 18:1/2:1/2:149:1/2:158; 1996.

Yang, T. C.; Stampfer, R. M.; Tobias, C. A. Radiation Studies on Sensitivity and Repair of Human mammary Epithelial Cell. Int. J. Radiat. Biol. 56:5:605-609; 1989.

Young, L.; Adamson, I. R. Epithelial-Fibroblast Interactions in Bleomycin-induced Lung Injury and Repair. Environ. Health Perspect. 101:1: 56-61; 1993.

FIGURE LEGENDS

1. NASA-designed HARV (high aspect ratio vessel) bioreactor used to culture suspension and anchorage-dependent cells.

2. Experimental design summarizing the development of three-dimensional, multi-cellular, bead-less tissue constructs in the HARV bioreactor.

3. Photomicrographs showing the three-dimensional growth of fibroblast cells on macroporous Cultispher-S microcarrier. A) Cultispher-S beads without cells (X200); B) Paraffin-embedded samples stained with H&E (X1000), and C) Movat (X1000); D) SEM of cells attaching to macroporous bead (X625); E) TEM of a fibroblast cells layered on the surface of bead (X 18,000) and F) MTT staining of viable cells growing on the bead (X200).

4. Histochemical analysis of cells cultured on macroporous beads in the bioreactor. A) Fibroblast cells (monoculture) stained with H&E on day 3; B) Movat on day 5 and C) day 8; D) Fibroblast and epithelial cells (coculture) stained with H&E on day 3; E) Movat on day 5 and F) day 8. (A-F, X1000)

5. Growth parameters of control and dispase-treated cocultures. Media samples of each culture were withdrawn daily to monitor (A) glucose concentration, (B) lactate concentration, and (C) pH levels.

6. Dispase treatment of spheroids in the HARV bioreactor. Analysis of spheroids following the 1st dispase treatment. A) MTT staining of viable cells (X200); B) Toludine stained section (X400); C) TEM showing cell detachment (X6000). Examination of spheroids following a 2nd dispase treatment. D) Light microscopy of treated spheroids (X100) and E)

X400; F) MTT staining of viable cells (X200); G) H&E staining of cells (X400) and H) X1000; I) TEM of treated samples (X10, 000). Examination of spheroid stability 1-week after dispase treatment. J) Phase contrast microscopy (200); K) Toludine staining (X200) and L) Movat staining (X1000).

7. Immunohistochemical analysis of cells stained for the presence of cytoskeletal proteins. A) Light microscopy of fibroblast cell monolayers (X200); B) Stained with vimentin (X200) and C) X400; D) Epithelial cell monolayer (X200); E) Stained for cytokeratin (X100) and F) 400X; (G) Stained for E-Cadherin (X200) and H) X400.

8. Fibroblast (monoculture) cells cultured on a Cultispher-S bead and (A) stained for vimentin (X400) and B) X1000; C) Dispase treated (X400). D) Fibroblast and epithelial (coculture) stained for vimentin (X400), E) X400 and F) X1000. G) Coculture stained for cytokeratin (X200), H) X1000 and I) X1000; J) Coculture stained for E-cadherin (X400).

9. Western blot analysis confirming the cross-reactivity of immunoreactive proteins for vimentin, cytokeratin, and E-cadherin. A) Endogenous vimentin expression in fibroblast cells, B) Epithelial cells and the expression of cytokeratin 7, C) cytokeratin 8, and D) cytokeratin 18. E) Expression of E-cadherin in epithelial cells.

10. Ultra-structural analysis of rat 2λ fibroblast (monoculture) cultivated in the HARV. A) SEM of monoculture, day 5 (X150); B) TEM of fibroblast (monoculture) cells growing on macroporous bead, day 3 (X3300); C) Dispase treated monoculture, SEM, day 5 (X1300); D) TEM, day 7 (X4500).

11. Comparison of electron micrographs of rat 2λ fibroblast and epithelial cells (coculture) cultured on a macroporous beads and epithelial cells only cultured on cytodex-3 microcarrier beads. Coculture A) SEM day 5 (X 200); B) TEM day 7 (X58,000); C) TEM

day 7 (X 78,000). TEM of epithelial cells cultured on cytodex-3 as a positive control (D) X 18,000, (E) X 42,000 and (F) X 3,000.

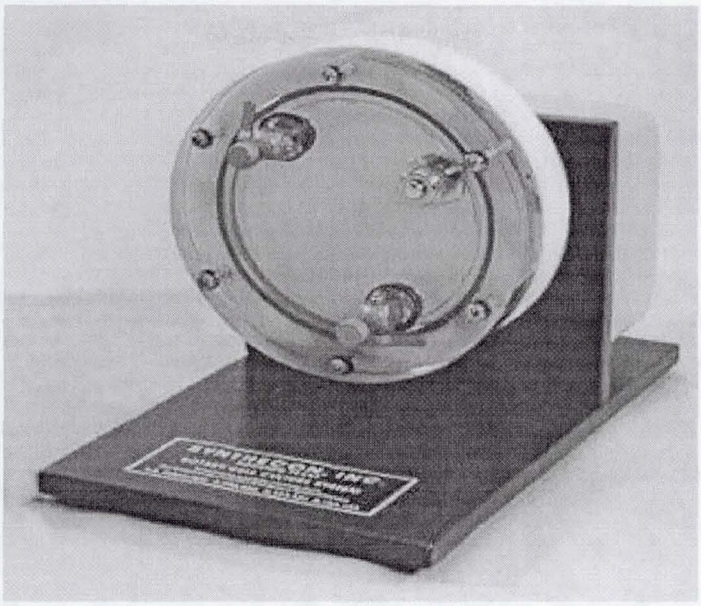

Figure 1

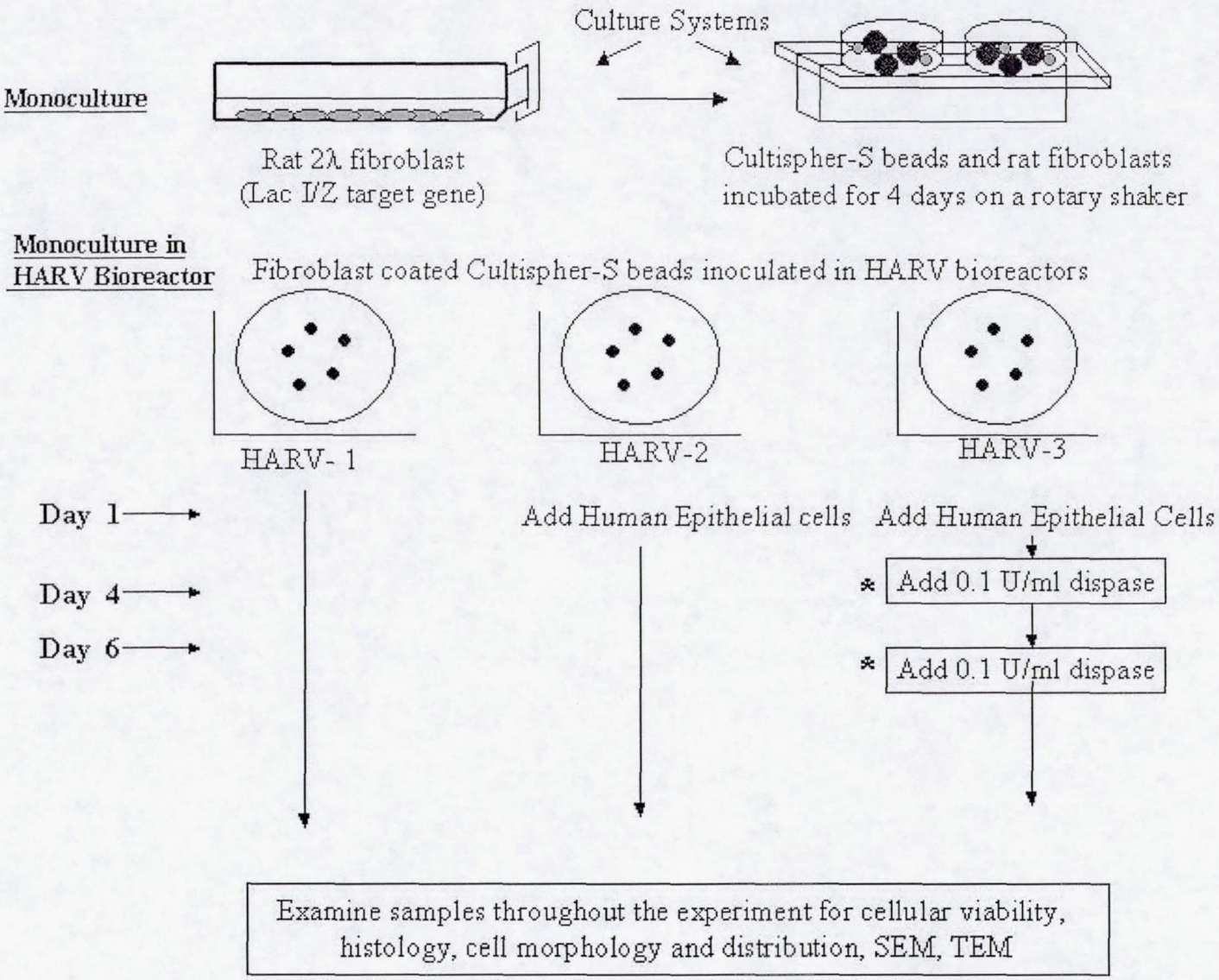
Culture Systems
Monoculture
Rat 2λ fibroblast
(Lac I/Z target gene)
Cultispher-S beads and rat fibroblasts
incubated for 4 days on a rotary shaker
Monoculture in
HARV Bioreactor
Fibroblast coated Cultispher-S beads inoculated in HARV bioreactors
HARV- 1
HARV-2
HARV-3
Day 1
Day 4
Day 6
Add Human Epithelial cells
Add Human Epithelial Cells
* Add 0.1 U/ml dispase
* Add 0.1 U/ml dispase
Examine samples throughout the experiment for cellular viability,
histology, cell morphology and distribution, SEM, TEM

Figure 2

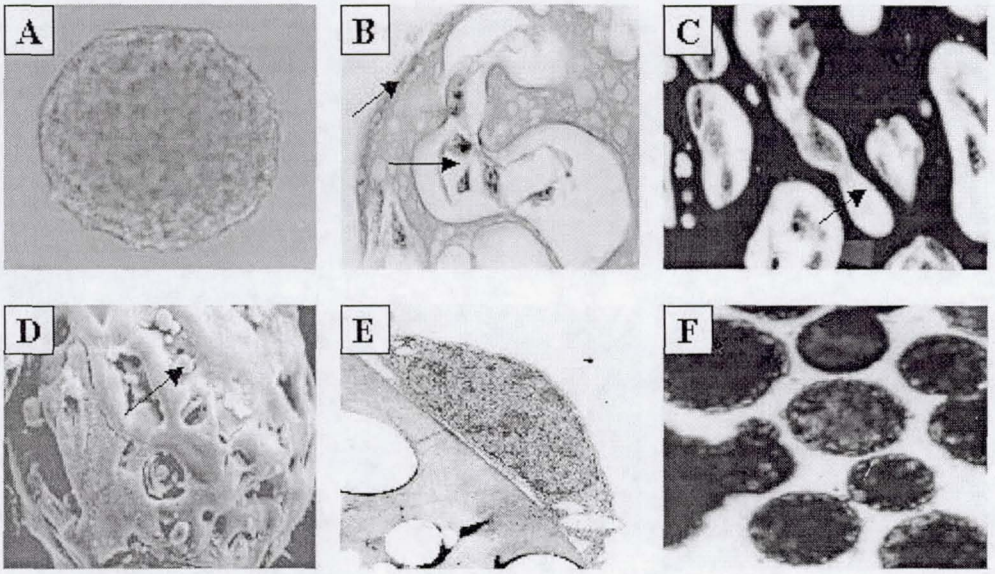

Figure 3

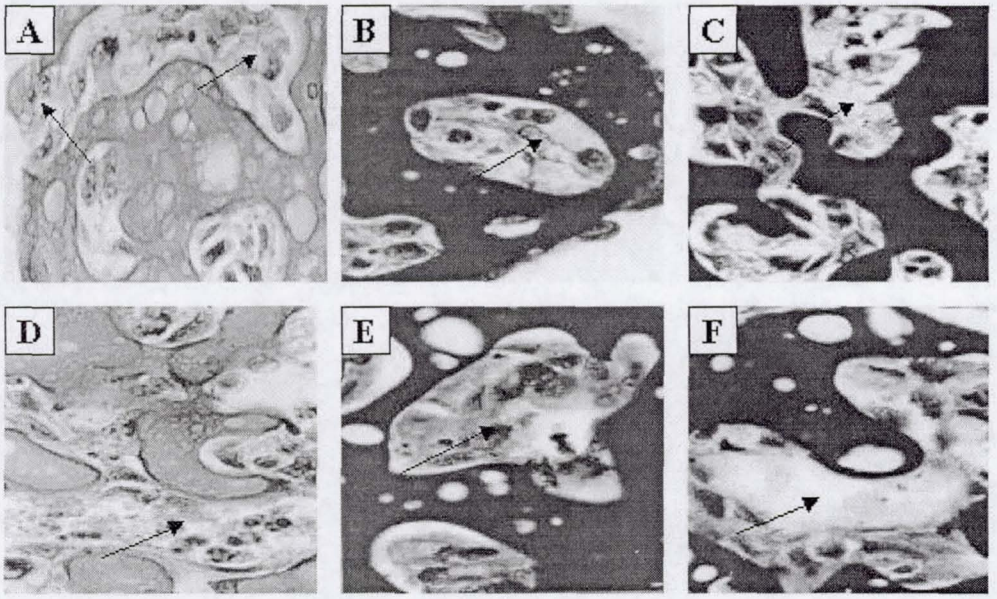

Figure 4

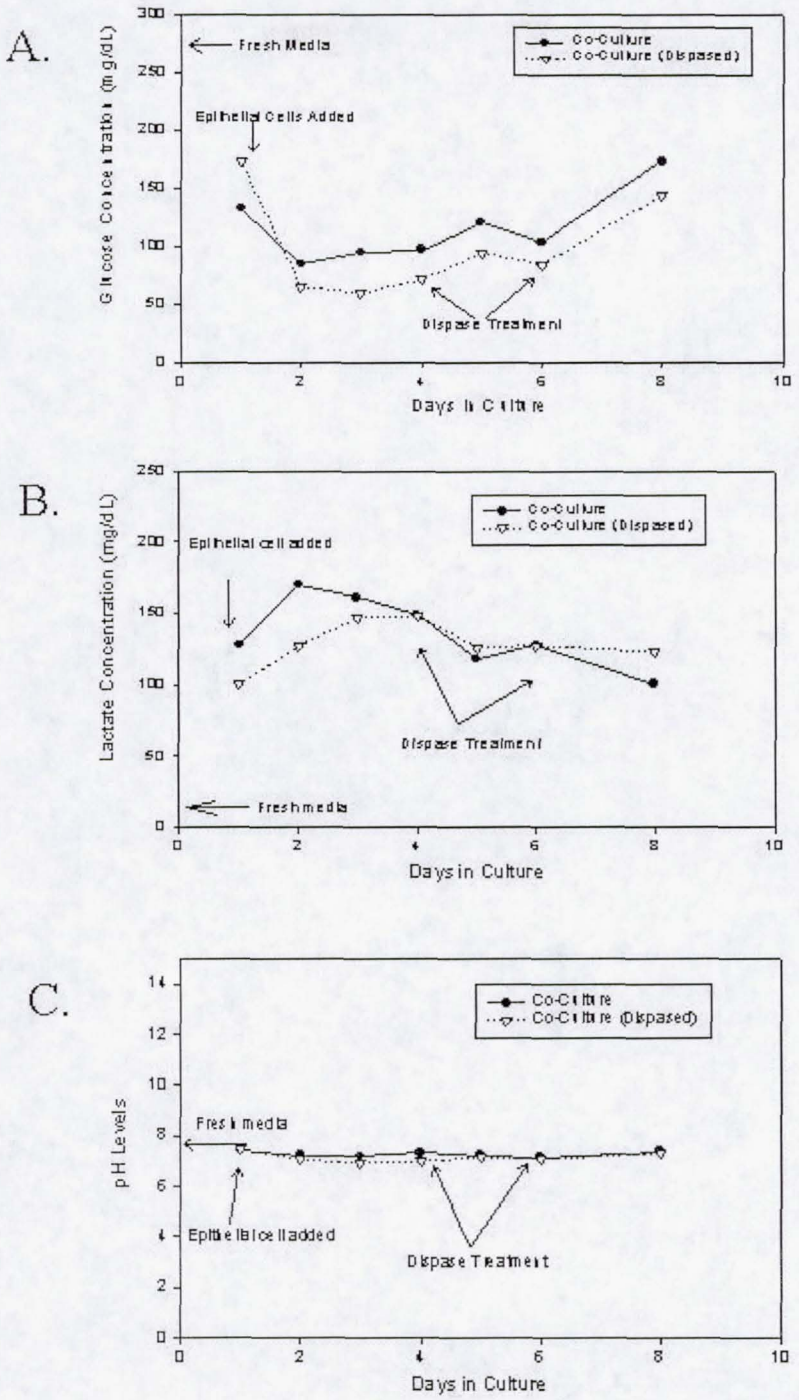
A.
Fresh Media
Co-Culture
Co-Culture (Dispased)
Epithelial Cells Added
Dispase Treatment
Glucose Concentration (mg/dL)
Days in Culture
B.
Co-Culture
Co-Culture (Dispased)
Epithelial cell added
Dispase Treatment
Fresh media
Lactate Concentration (mg/dL)
Days in Culture
C.
Co-Culture
Co-Culture (Dispased)
Fresh media
Epithelial cell added
Dispase Treatment
pH Levels
Days in Culture

Figure 5

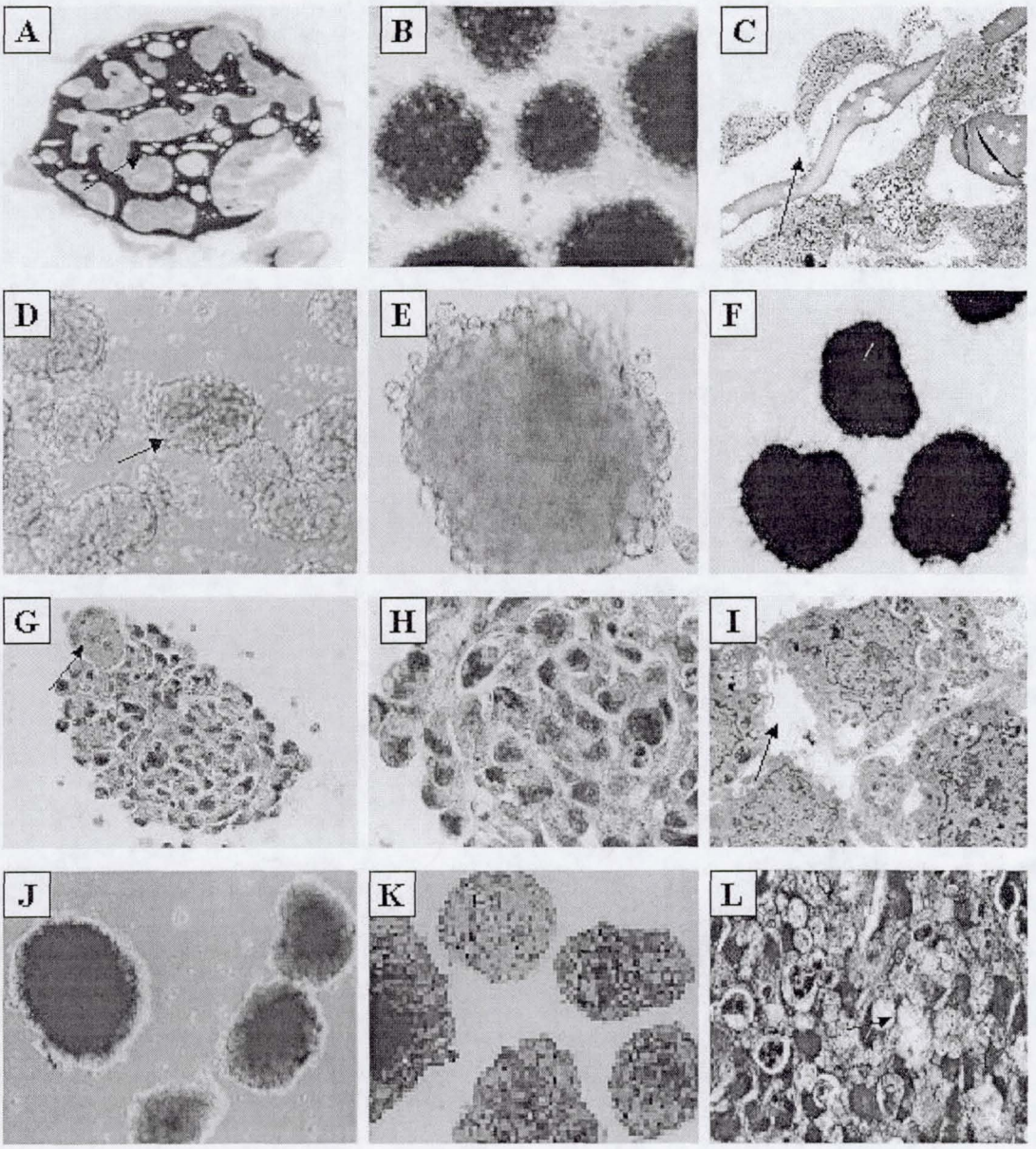

Figure 6

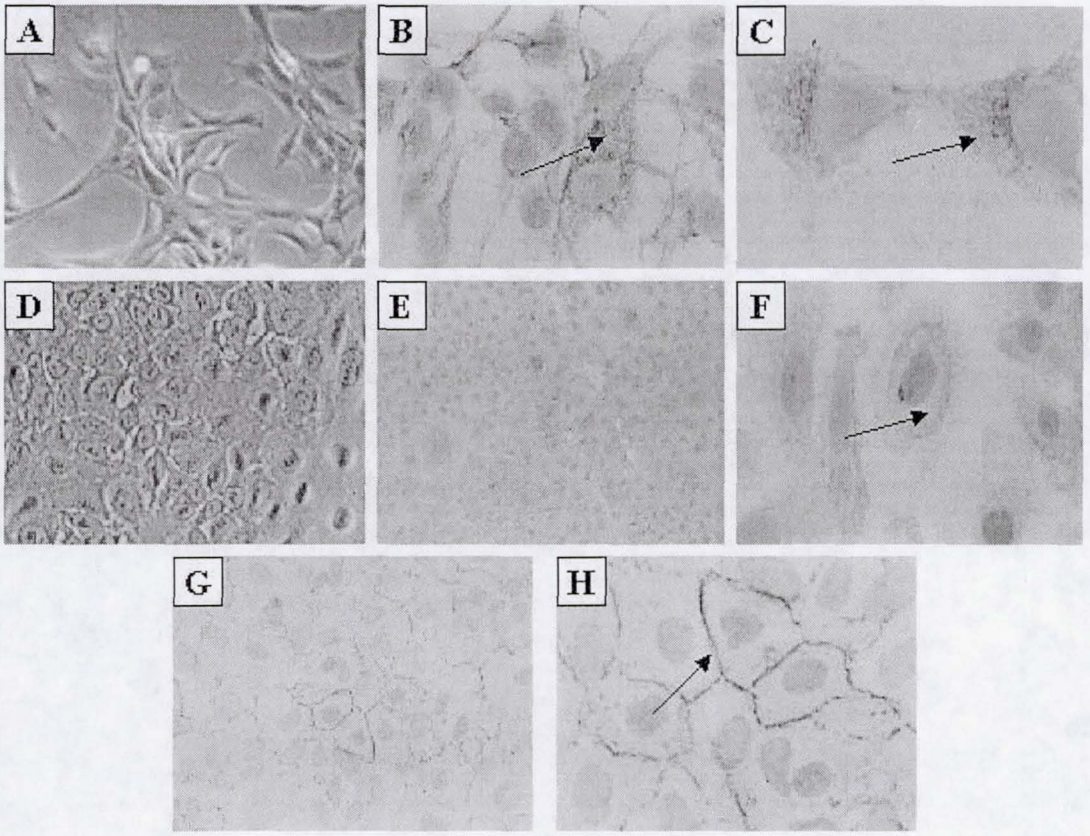

Figure 7

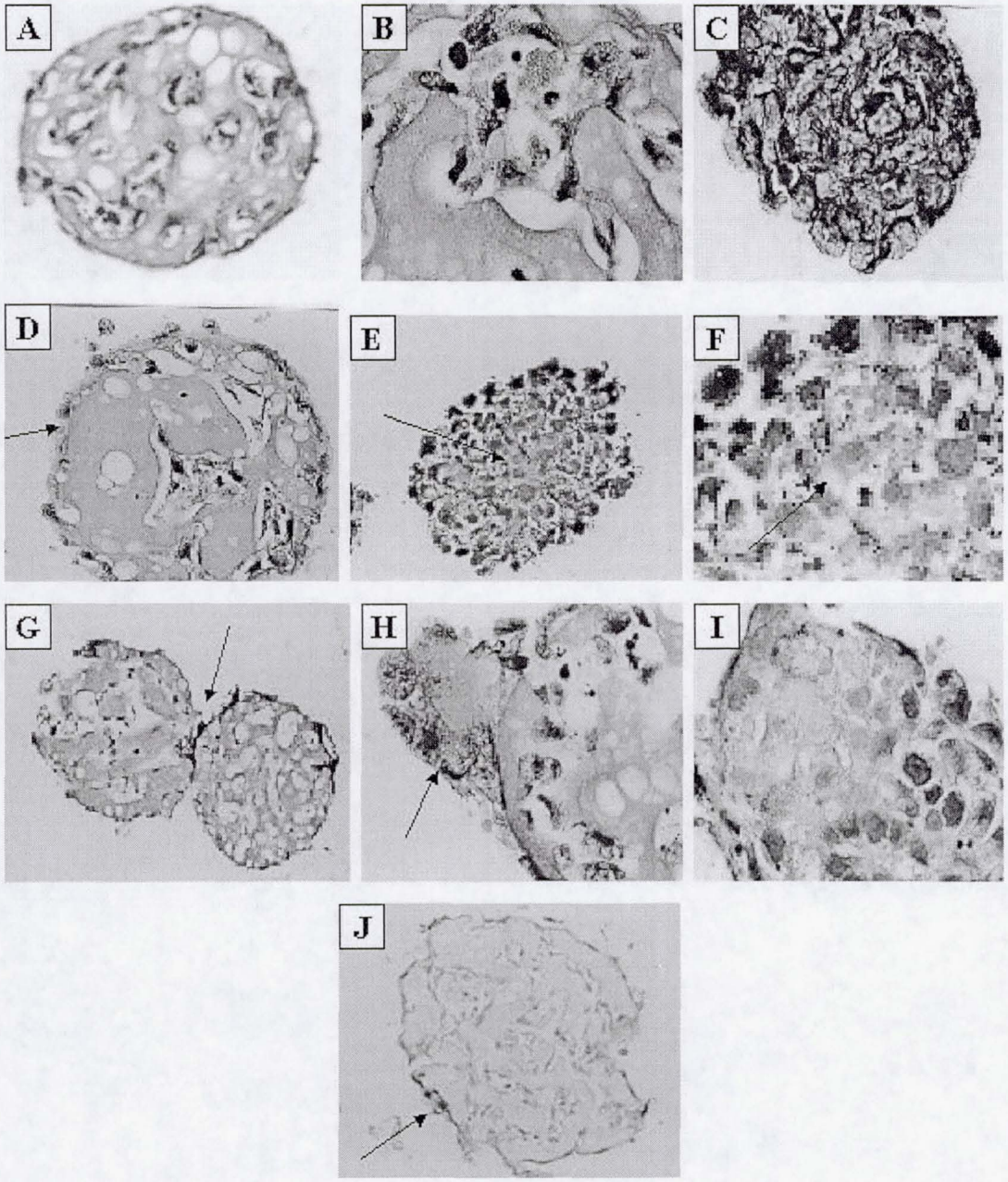

Figure 8

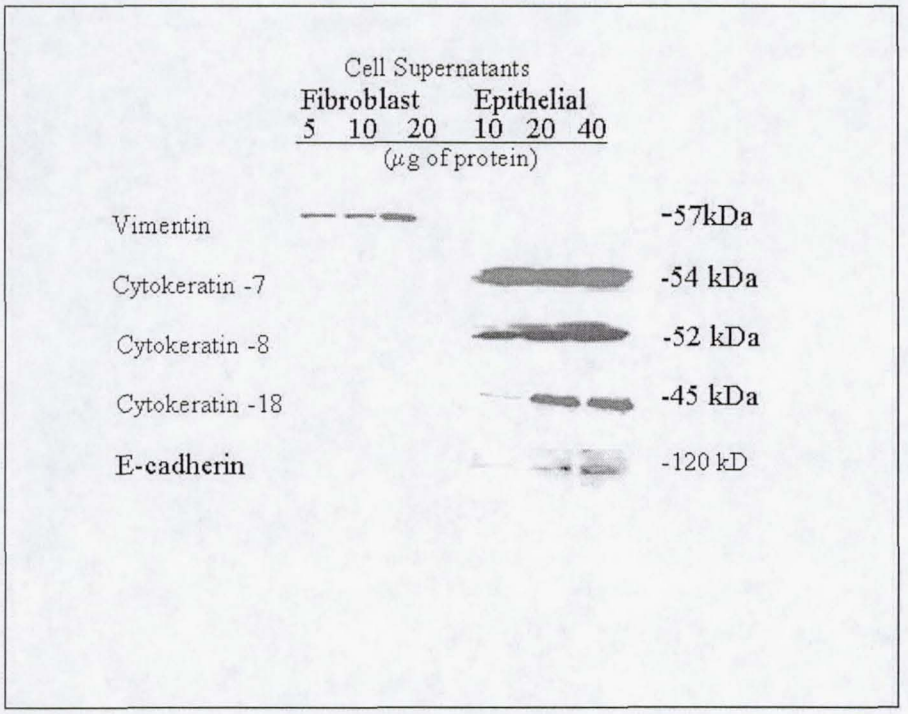

Figure 9

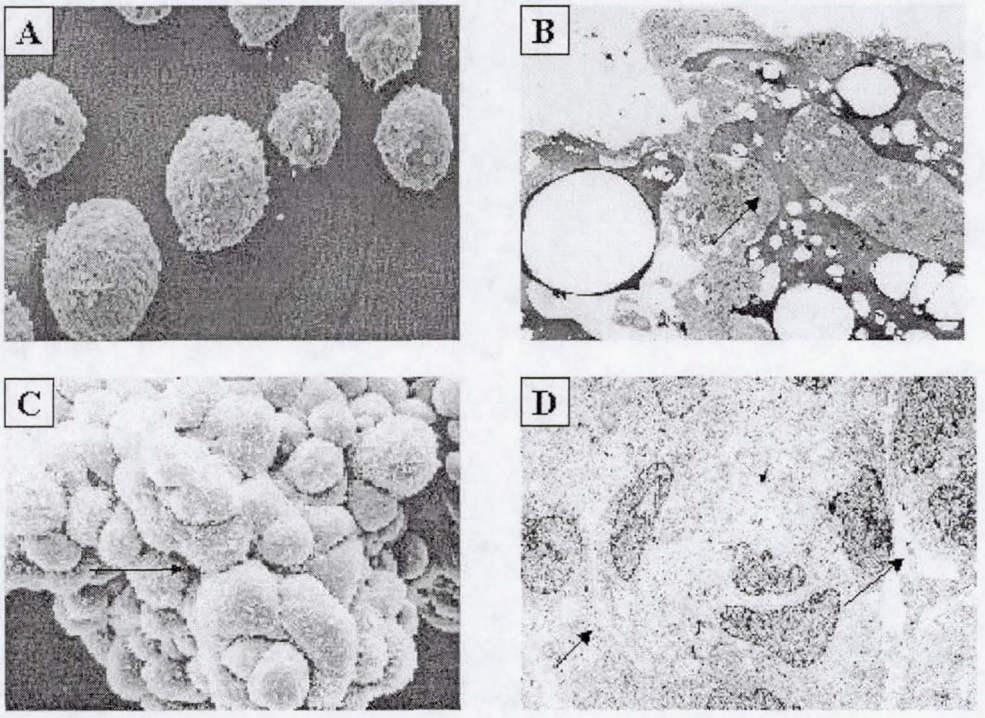

Figure 10

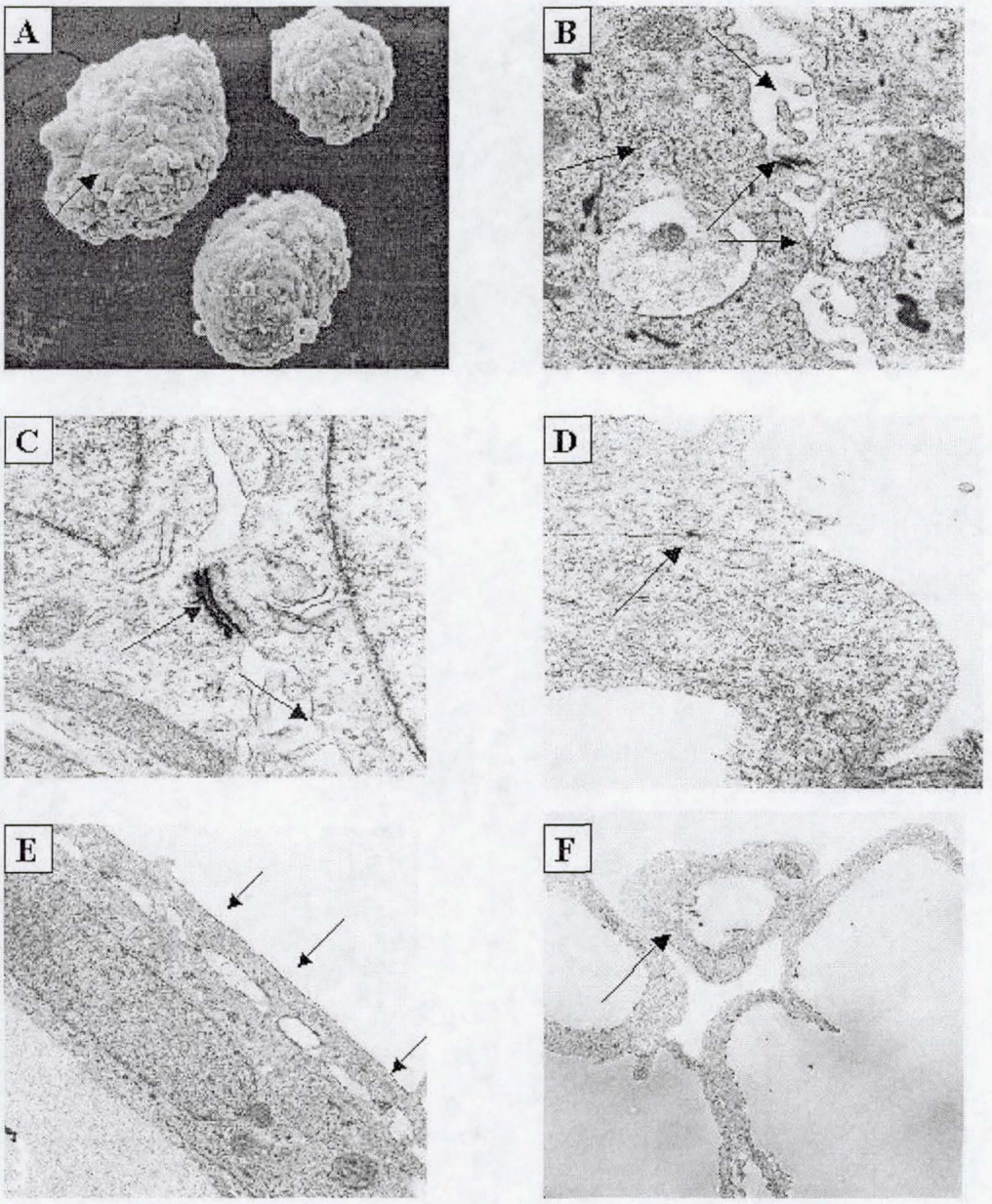

Figure 11